Available online at www.sciencedirect.com
SCIENCE DIRECT®
ELSEVIER
International Journal of Thermal Sciences 44 (2005) 598–607
International Journal of Thermal Sciences
www.elsevier.com/locate/ijts

Investigation of heat transfer and exergy loss in a concentric double pipe exchanger equipped with swirl generators

Ebru Kavak Akpinar *, Yasar Bicer

Mechanical Engineering Department, Firat University, 23279 Elazig, Turkey

Received 3 May 2004; accepted 22 November 2004

Abstract

In this study, the effect on heat transfer rates, friction factor and exergy loss of swirl generators with holes for the entrance of fluid were investigated by placing them at the entrance section of inner pipe of heat exchanger. Various swirl generators having circular holes at different number and diameter were used. Hot air and cold water were passed through the inner pipe and annulus, respectively. Experiments were carried out for both parallel and counter flow models of the fluids at Reynolds numbers between 8500–17 500. Heat transfer, friction factor and exergy analyses were made for the conditions with and without swirl generators and compared to each other. Some empirical correlations expressing the results were also derived and discussed. It was observed that the Nusselt number could increase up to 130% at a value of about 2.9 times increase in the friction factor by giving rotation to the air with the help of the swirl elements. The increase the dimensionless exergy loss was about 1.25 times in comparison with that for the inner pipe without swirl generators.

Keywords: Concentric heat exchanger; Exergy loss; Friction factor; NTU; Swirl generator

1. Introduction

Heat transfer enhancement at heat exchangers may be achieved by numerous techniques, and these techniques can be classified into three groups: passive, active and compound techniques [1,2]. In the active techniques, heat transfer is improved by giving additional flow energy into the fluid. In the passive techniques, however, this improvement is acquired without giving any extra flow energy. In the compound techniques, two or more of the active or passive techniques may be utilized simultaneously to produce an enhancement that is much higher than the techniques operating separately [2].

The applications of swirling flow, or its effects, to the fluid for increasing heat transfer can be divided into two groups. One is the so-called non-decaying swirling flow type in which turbulators located through or in certain distances in the flow area continuously generate swirling flow. In the second type, which is called decaying flow, the swirling effect to the fluid is only given in the inlet flow area, and then, the fluid flows freely in the following area. In the case of swirling flows, the heat transfer and pressure losses should be carefully analyzed and optimized for the energy economy aspects because they bring additional pumping power and construction costs, all increasing the total cost of a heat exchanger [3,4].

Exergy analysis can reveal whether or not and by how much it is possible to design more efficient thermal systems by reducing the sources of existing inefficiencies. Increased efficiency can often contribute in a major way to achieving energy security in an environmentally acceptable way by the direct reduction of irreversibilities that might otherwise have occurred. This makes exergy one of most powerful tools to provide optimum conditions [5,6].

Turbulent swirling flows in a pipe are poorly understood, although a number of studies of these flows have been reported in the literature [2–4,7–14]. Many authors consider that swirling flow of a fluid through a pipe is highly complex

* Corresponding author. Tel.: +90-424-2370000/5343; Fax: +90-424-2415526.

E-mail addresses: eakpinar@firat.edu.tr (E. Kavak Akpinar), ybicer@firat.edu.tr (Y. Bicer).

1290-0729/$ – see front matter
doi:10.1016/j.ijthermalsci.2004.11.001

Nomenclature

A	heat transfer area	m^2
A_i	inner pipe inside surface area	m^2
A_o	inner pipe outer surface area	m^2
C_p	specific heat capacity	$J{\cdot}kg^{-1}{\cdot}°C^{-1}$
C_{max}	maximum heat capacity	$W{\cdot}K^{-1}$
C_{min}	minimum heat capacity	$W{\cdot}K^{-1}$
C_r	heat capacity ratio	
d	diameter of inner pipe	m
D	diameter of outer pipe	m
d_s	diameter of holes on the swirl elements	m
e	dimensionless exergy loss	
Ex	exergy	
$\dot{E}x_{loss}$	exergy loss	W
f	friction factor	
h	specific enthalpy	$J{\cdot}kg^{-1}$
H_c	average heat transfer coefficient of cold fluid	$W{\cdot}m^{-2}{\cdot}K^{-1}$
H_h	average heat transfer coefficient of hot fluid	$W{\cdot}m^{-2}{\cdot}K^{-1}$
j	total number of holes on the swirl elements	
k	thermal conductivity of fluid	$W{\cdot}m^{-1}{\cdot}K^{-1}$
L	length of pipe	m
$\dot{m}$	mass flow rate	$kg{\cdot}s^{-1}$
n	number constants	
N	number of observations	
Nu	Nusselt number	
NTU	number of heat transfer units	
Pr	Prandtl number	
$\dot{Q}$	heat transfer rate	W
R	correlation coefficients	
Re	Reynolds number	
$RMSE$	root mean square error analysis	
s	specific entropy	$J{\cdot}kg^{-1}{\cdot}K^{-1}$
T	temperature	°C
T_r	temperature ratio	
U	overall heat transfer coefficient	$W{\cdot}m^{-2}{\cdot}K^{-1}$
U_m	average fluid velocity	$m{\cdot}s^{-1}$
W	total uncertainty in the measurement	
$\dot{W}$	work	W
Y_{exp}	experimental value	
Y_{pre}	predicted value	
ΔP	pressure drop	Pa
ΔT_{li}	logarithmic temperature difference between wall and air temperature	K
ΔT_{lo}	logarithmic temperature difference between wall and water temperature	K
ΔT_L	logarithmic mean temperature difference	K

Greek symbols

ρ	density of fluid	$kg{\cdot}m^{-3}$
ε	effectiveness	
χ^2	chi-square	

Subscripts

c	cold
CH	chemical
e	environmental condition
h	hot
i	inlet condition or inner
KN	kinetic
loss	loss
max	maximum
min	minimum
o	outlet condition or outer
PH	physical
PT	potential

turbulent flows in which a fluid element moves along helical paths and regions of back-flow may appear near the axis of the pipe, rather than a motion of fluid with axial and tangential velocity components. For this reason, there is still no generalized method to predict this kind of flow imposed by various swirl generators [10,13]. The effect of swirling flow on heat transfer, however, may be determined using global expressions.

Although numerous studies on the energy and exergy analysis of thermal systems and applications have recently been undertaken by some researchers, e.g., [5,6,15–20], very few papers have appeared on exergy analyses of concentric heat exchanger with swirl generator, e.g., [3,4]. It is therefore the purpose of this work to study the effect of a number of different swirl generators on the heat transfer, friction factor and dimensionless exergy loss. Swirl generators in this work have got different properties from the works at the literature. These elements containing holes for the passage of fluid into the tube are assumed to impose swirling motion to the fluid. It is aimed to increase heat transmission by imposing swirl to the fluid in the entrance section of a double-pipe concentric heat exchanger which has been used extensively due to its easy construction with no movable parts and low cost. Therefore, this study is different from others in the scope of heat transfer and exergy analysis of such as system.

2. Experimental set-up and procedure

The experimental set-up is shown in Fig. 1. The dimensions of inner and outer pipes of the heat exchanger are: $d_i = 35$ mm, $d_o = 41$ mm, $L_i = 810$ mm; $D_i = 70$ mm, $D_o = 75$ mm and $L_o = 750$ mm. Heat exchanger has portable lids of 150 mm length at both ends. Hot air was passed through the inner pipe, while cold water was flowing through the annulus. Heating of the air was achieved with an electrical

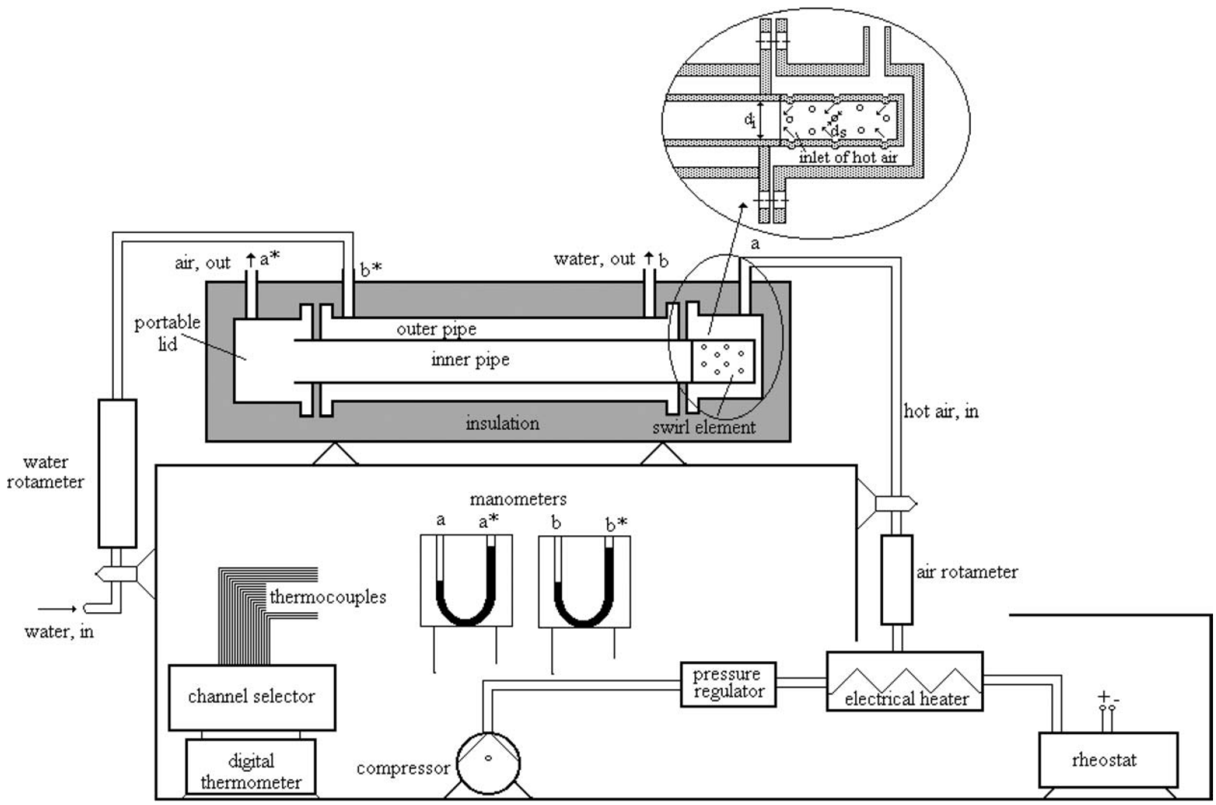

Fig. 1. Experimental set-up.

heater at the entrance and its power was adjusted with a rheostat [13].

Various swirl generators, which have given swirling to the fluid, have been prepared for experimental evaluation. The elements were made cylindrical shape in 100 mm length and 42 mm diameter from thin galvanized iron plates. These elements are lid-shaped parts containing circular holes in different diameter and number, they can be placed and removed easily on the entrance section of the inner pipe. The holes were drilled in an angle different from the normal to the surface. The holes were connected to the pipes with angle of 45° and length of 10 mm. They have four rows of 3, 6 or 9 mm diameter holes for air entrance to the inner pipe of heat exchanger. Each row has three, four or five holes. That is to say, each of swirl generators has 12, 16 and 20 holes. The holes were arranged in a zigzag line as shown in Fig. 1. Separate experiments were also conducted for this heat exchanger without using these swirl generators [13].

The inlet and outlet temperatures of the fluids, the temperatures of the points on the inner pipe wall and ambient temperature were measured with Iron–Constantan thermocouples. The temperatures were read with a multi-channel digital thermometer. Pressure losses were determined by using U manometers that were filled with water for the air side and with mercury for the water side. The air was supplied from an air compressor. The flow rates of air and water were adjusted with valves and measured with rotameters. In order to keep constant airflow rates at various levels, a pressure regulator was also used. The experimental work was repeated for both parallel and countercurrent flow modes and for the swirl elements having different arrangements of holes at various fluids Reynolds numbers [13].

3. Experimental uncertainty

All instruments and measurements have certain general characteristics. An understanding of these common qualities is the first step towards accurate measurement. Errors and uncertainties are inherent in both the instrument and the process of making the measurement, and too much reliance should not be placed on any single reading from one affected by the environment. Final accuracy depends on a sound program and on correct methods for taking reading on the proper instruments. When readings are repeated, they tend to produce a band of results rather than a point or a line. Errors and uncertainties in the experiments can arise from instrument selection, instrument condition, instrument calibration, environment, observation, and reading, and test planning [13,21]. In the experiments of heat transfer enhancements in a concentric double pipe exchanger equipped with swirl elements, the temperatures, pressure drops, flow rates were measured with appropriate instruments. During the measurements of the parameters, the uncertainties occurred were presented in Table 1. Considering the relative errors in the individual factors denoted by

Table 1
Uncertainties of the parameters during the experiments of heat transfer enhancements in a concentric double pipe exchanger equipped with swirl elements

Parameter	Unit	Comment
Uncertainty in the temperature measurement		
Hot fluid inlet temperature	°C	±0.380
Hot fluid outlet temperature	°C	±0.380
Cold fluid inlet temperature	°C	±0.380
Cold fluid outlet temperature	°C	±0.380
Inner pipe wall temperature	°C	±0.628
Ambient temperature	°C	±0.380
Uncertainty in the measurement of pressure drop		
Air side	mmSS	±0.282
Water side	mmHg	±0.282
Uncertainty in the measurement of volume flow rate		
Air	$m^3 \cdot h^{-1}$	±0.2
Water	$m^3 \cdot h^{-1}$	±0.2
Uncertainty in reading values of table ($\rho, C_p, k \ldots$)	%	±0.1–0.2

x_n, error estimation was made using the following equation [22]:

$$W = \left[(x_1)^2 + (x_2)^2 + \cdots + (x_n)^2\right]^{1/2} \tag{1}$$

4. Analysis

4.1. Heat transfer

The efficiency of a heat exchanger is defined as the ratio of the heat transferred to maximum heat transfer

$$\varepsilon = \frac{\dot{Q}}{\dot{Q}_{\max}} \tag{2}$$

the heat transferred from the hot air is given as

$$\dot{Q}_h = \dot{m}_h C_{p_h}(T_{hi} - T_{ho}) = H_h A_i \Delta T_{li} \tag{3}$$

and the heat received by the cold water is

$$\dot{Q}_c = \dot{m}_c C_{p_c}(T_{co} - T_{ci}) = H_c A_o \Delta T_{lo} \tag{4}$$

The difference between these two rates shows the convective heat loss from the exchanger, which may be assumed to be negligible here

$$\dot{Q}_{loss} = \dot{Q}_h - \dot{Q}_c \tag{5}$$

The Nusselt number, in terms of the air side average heat transfer coefficient, is

$$Nu = \frac{H_h d_i}{k} \tag{6}$$

On the other hand, the overall heat transfer coefficient may be defined by the equation

$$\dot{Q}_h = U_i A_i \Delta T_L \tag{7}$$

where, ΔT_L is the logarithmic mean temperature difference over the exchanger. The overall heat transfer coefficient may be calculated using the measured wall temperatures of the inner pipe (arithmetical average of five point) and Eqs. (3) and (4). Eq. (7) may then be used to control the results of calculation [23,24].

The following equation can be used to calculate the maximum heat given

$$\dot{Q}_{\max} = C_{\min}(T_{hi} - T_{ci}) = \dot{m}_h C_{p_h}(T_{hi} - T_{ci}) \tag{8}$$

The number of heat transfer units, *NTU*, is expressed in terms of thermal capacity,

$$NTU = \frac{UA}{C_{\min}} \tag{9}$$

4.2. Exergy analysis

Exergy is the maximum amount of work obtained theoretically at the end of a reversible process in which equilibrium with the environment is attained. According to this definition, the reference environment conditions must be known to calculate exergy. Temperature of the reference environment in this work varied between 20 with 22 °C (ambiance temperature).

A heat exchanger is characterized by two types of losses: temperature difference and frictional pressure drop in the pipe. These losses refer to irreversibility quantity, and some methods have been devised for minimizing these losses [26,27]. However, in this study, the exergy analysis does not include friction (or pressure drop) irreversibilities and based only heat transfer irreversibilities.

The total exergy of a system *Ex* can be divided into four components, namely

(i) physical exergy Ex^{PH},
(ii) kinetic exergy Ex^{KN},
(iii) potential exergy Ex^{PT}, and
(iv) chemical exergy Ex^{CH} [25].

$$Ex = Ex^{PH} + Ex^{KN} + Ex^{PT} + Ex^{CH} \tag{10}$$

Physical exergy is the majority of the heat exchanger system. Therefore, chemical exergy, potential exergy, nuclear exergy, magnetic exergy and kinetic exergy (kinetic energy) were neglected in this study.

In this case, the exergy balance in a steady open system can be written as follows [28]:

$$\sum \dot{E}x_i - \sum \dot{E}x_o + \sum \dot{E}x_{product} = 0 \tag{11}$$

The lost work as being described between difference of maximum work with real work

$$\dot{W}_{lost} = \dot{W}_{\max} - \dot{W}_{actual} = \dot{E}x_{loss} \tag{12}$$

and this expression is equal to the exergy loss. Therefore, the exergy loss in open systems is

$$\dot{E}x_{loss} = \sum \dot{m}_i(h_i - T_e s_i) - \sum \dot{m}_o(h_o - T_e s_o) + \sum \dot{Q}\left(1 - \frac{T_e}{T}\right) - \dot{W} \tag{13}$$

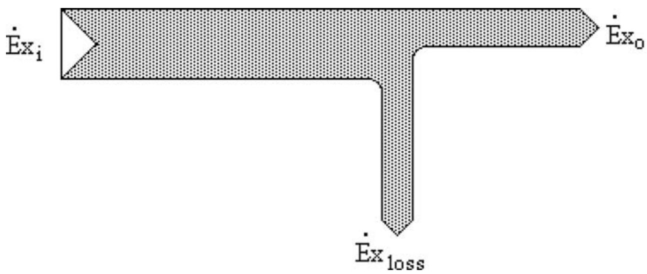

Fig. 2. Exergy band diagram for heat exchanger.

Fig. 2 shows exergy band diagram for heat exchanger. The exergy loss in an open system heat exchanger is given as

$$\dot{E}x_{\text{loss}} = \dot{m}_{\text{c}}(h_{\text{ci}} - T_{\text{e}}s_{\text{ci}}) + \dot{m}_{\text{h}}(h_{\text{hi}} - T_{\text{e}}s_{\text{hi}}) - \dot{m}_{\text{c}}(h_{\text{co}} - T_{\text{e}}s_{\text{co}}) - \dot{m}_{\text{h}}(h_{\text{ho}} - T_{\text{e}}s_{\text{ho}}) \tag{14}$$

and rearranging this equation gives the following:

$$\dot{E}x_{\text{loss}} = \dot{m}_{\text{c}}(h_{\text{ci}} - h_{\text{co}}) + \dot{m}_{\text{h}}(h_{\text{hi}} - h_{\text{ho}}) + T_{\text{e}}\big[\dot{m}_{\text{c}}(s_{\text{co}} - s_{\text{ci}}) + \dot{m}_{\text{h}}(s_{\text{ho}} - s_{\text{hi}})\big] \tag{15}$$

In a heat exchanger, the heat given by the hot fluid becomes equal to the heat taken by the could fluid if the heat losses $\dot{Q}_{\text{loss}}$ are assumed to be negligible

$$\dot{Q} = \dot{m}_{\text{h}}(h_{\text{hi}} - h_{\text{ho}}) = \dot{m}_{\text{c}}(h_{\text{ci}} - h_{\text{co}}) \tag{16}$$

By using Eq. (15), the following equation can be derived

$$\dot{E}x_{\text{loss}} = T_{\text{e}}\big[\dot{m}_{\text{c}}(s_{\text{co}} - s_{\text{ci}}) + \dot{m}_{\text{h}}(s_{\text{ho}} - s_{\text{hi}})\big] \tag{17}$$

If entropy gradients of hot and cold fluids are expressed in terms of specific heats in constant pressure

$$s_{\text{co}} - s_{\text{ci}} = C_{p_{\text{c}}} \ln(T_{\text{co}}/T_{\text{ci}})$$
$$s_{\text{ho}} - s_{\text{hi}} = C_{p_{\text{h}}} \ln(T_{\text{ho}}/T_{\text{hi}}) \tag{18}$$

and inserting Eq. (18) into Eq. (17),

$$\dot{E}x_{\text{loss}} = T_{\text{e}}\big[\dot{m}_{\text{h}}C_{p_{\text{h}}} \ln(T_{\text{ho}}/T_{\text{hi}}) + \dot{m}_{\text{c}}C_{p_{\text{c}}} \ln(T_{\text{co}}/T_{\text{ci}})\big] \tag{19}$$

Thermal capacities of hot and cold fluids and ratio of capacities are

$$C_{\text{h}} = \dot{m}_{\text{h}}C_{p_{\text{h}}}, \qquad C_{\text{c}} = \dot{m}_{\text{c}}C_{p_{\text{c}}}$$
$$C_{\text{r}} = C_{\min}/C_{\max} \tag{20}$$

If we assume that the thermal capacity of the hot fluids is minimum, exergy loss can be written as follows:

$$\dot{E}x_{\text{loss}} = T_{\text{e}}\big[C_{\min} \ln(T_{\text{ho}}/T_{\text{hi}}) + C_{\max} \ln(T_{\text{co}}/T_{\text{ci}})\big] \tag{21}$$

and if the following relations are described

$$T_{\text{r}} = T_{\text{hi}}/T_{\text{ci}}$$
$$\varepsilon = \frac{\dot{Q}}{\dot{Q}_{\max}} = \frac{C_{\max}(T_{\text{co}} - T_{\text{ci}})}{C_{\min}(T_{\text{hi}} - T_{\text{ci}})} = \frac{C_{\min}(T_{\text{hi}} - T_{\text{ho}})}{C_{\min}(T_{\text{hi}} - T_{\text{ci}})} \tag{22}$$

and inserting Eqs. (20), (22) into Eq. (21), the exergy loss equation is obtained as follows:

$$\dot{E}x_{\text{loss}} = T_{\text{e}}\left[C_{\min} \ln\left[1 - \varepsilon\left(1 - \frac{1}{T_{\text{r}}}\right)\right] + C_{\max} \ln\big[1 + \varepsilon C_{\text{r}}(T_{\text{r}} - 1)\big]\right] \tag{23}$$

If Eq. (23) is divided by $(T_{\text{e}}C_{\min})$, dimensionless exergy loss expression can be written as follows:

$$e = \frac{\dot{E}x_{\text{loss}}}{T_{\text{e}}C_{\min}} = \ln\left[1 - \varepsilon\left(1 - \frac{1}{T_{\text{r}}}\right)\right] + \frac{1}{C_{\text{r}}} \ln\big[1 + \varepsilon C_{\text{r}}(T_{\text{r}} - 1)\big] \tag{24}$$

4.3. Friction factor

The experimental pressure drops in the inner test pipe of concentric heat exchanger were measured for air side conditions and were arranged in non-dimensional form by using the following equation:

$$f = \frac{\Delta P}{(L_{\text{i}}/d_{\text{i}})\rho U_{\text{m}}^2/2} \tag{25}$$

5. Regression analysis

The regression analysis was performed using the Statistica computer program. The correlation coefficient (R), the reduced chi-square (χ^2) and root mean square error analysis $(RMSE)$ were used to determine the quality of the developed relation. These parameters can be calculated as follows [21]:

$$\chi^2 = \frac{\sum_{i=1}^{n}(Y_{\text{exp},i} - Y_{\text{pre},i})^2}{N - n} \tag{26}$$

$$RMSE = \left[\frac{1}{N}\sum_{i=1}^{N}(Y_{\text{pre},i} - Y_{\text{exp},i})^2\right]^{1/2} \tag{27}$$

6. Results and discussion

With the values obtained from the experimental data in inner pipe, the changes in the Nusselt numbers with the Reynolds numbers were drawn for various swirl generators containing circular holes at different diameter and number, as shown in Fig. 3. The experiments were performed for both counter and parallel flow mode, and results were compared to those obtained from the empty tube and Dittus–Boelter correlation $Nu = 0.023Re^{0.8}Pr^{0.4}$ (describes non-swirling flow in the smooth-tube) [29]. Indeed, the empty tube has the tangential inlet, which generates the swirl flow. The swirl flow induced by the step-shape distribution of the vorticity has a set of axial velocity profiles under the same Reynolds and swirl numbers. This is the main distinction between flows with and without swirling [14].

It is clear from Fig. 3 that the highest Nusselt number was achieved with the heat exchanger operated in a counter-flow

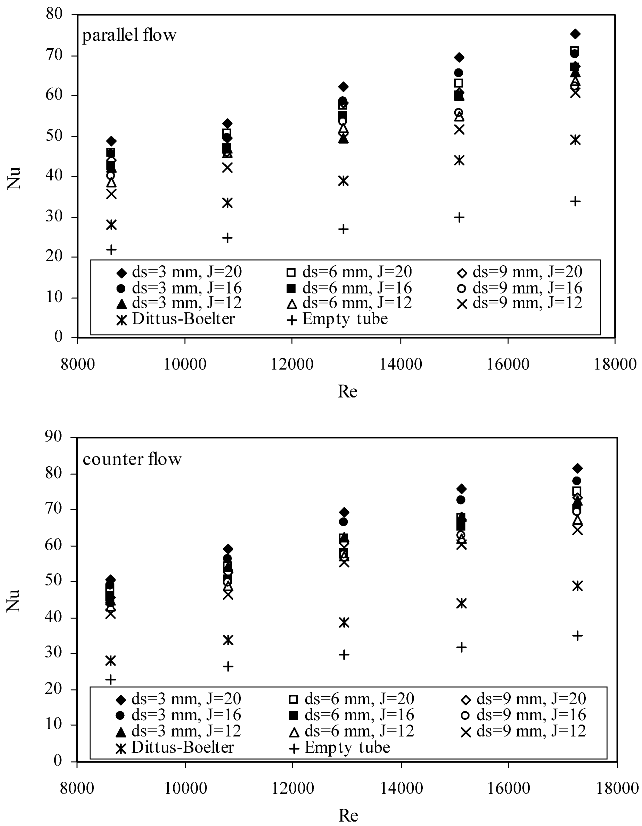

Fig. 3. The variation of Nusselt number with Reynolds number in the parallel and counter.

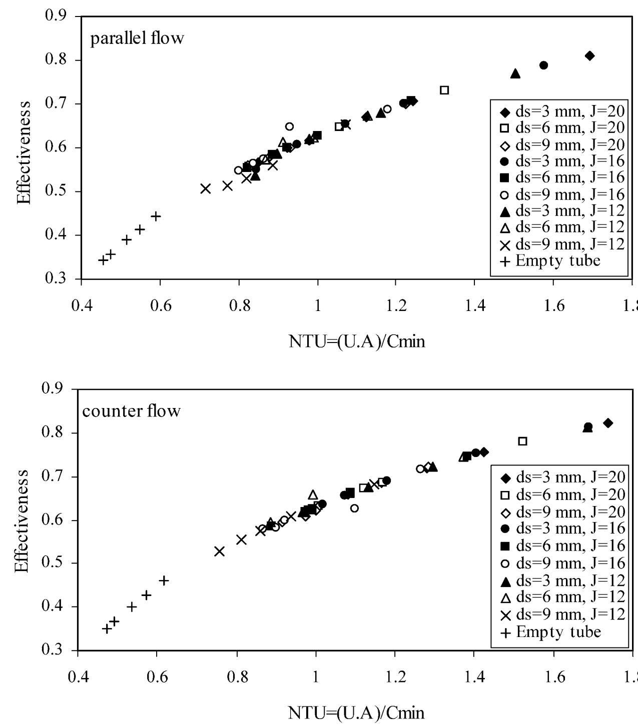

Fig. 4. The variation of effectiveness with *NTU* in the parallel and counter.

mode and equipped by a swirl generator having 20 circular holes with 3 mm diameter. In this run an increase in the Nusselt number was obtained up to 130% compared to a heat exchanger with the empty tube. While the increase in the Nusselt number was 113% at swirl generator having 20 circular holes with 6 mm diameter, the increase was 109% at 9 mm diameter. In all cases, the swirling flow gave higher values of Nusselt number than those for the empty tube and the Dittus–Boelter regime (non-swirling flow). However, swirling flow could not only to increase heat transfer, but to decrease it as well. Because, two types of vortex structures can exist in the swirl flows with the same integral characteristics: vortices with left-handed and right-handed helical symmetry. Left-handed helical vortexes generate wake-like swirl flows and increase heat transfer in comparison with the axial flow. Right-handed vortex structures generate jet-like swirl flows and can diminish heat transfer in comparison with the developing axial flow having the same *Re* number [14]. Heat transfer enhancement in this study is a consequence of formation of the swirl flow with left-handed helical vortex in pipe and the increase of the axial velocity near the wall. Because, the increase of the near-wall velocity produces larger temperature gradients and higher heat transfer rate. It was determined that heat transfer rates increased with decreasing diameter and with increasing number of holes on the swirl generators used in the experiments. The effect of the holes diameter on the heat transfer may be explained in terms of turbulent intensities. The turbulent intensities in the initial parts of the inner pipe must be higher for smaller diameter holes. Mutual holes of swirl generators may also affect heat transfer by promoting decay of swirls in the entrance section of the inner pipe. However, from these figures, it is also seen that the effect of swirl generators on the heat transfer is less for low values of the Reynolds numbers. Thus, the relative increase in the Nusselt number was low at smaller Reynolds numbers, while it became greater at high Reynolds numbers. The values given above are of a heat exchanger equipped with swirl generators having 20 holes and operated in counter-flow mode. The enhancements in heat transfer rates decreased with decreasing number of holes in the rows and 5–10% smaller for 16 holes than those with 20 holes and 5–10% smaller for 12 holes than those with 16 holes. The improvements for parallel flow showed a parallel trend, but, the values found for parallel flow mode were also 5–10% lower than corresponding values obtained in counter-flow mode as seen in Fig. 3.

Fig. 4 shows the changes of the effectiveness with *NTU* for various swirl generators containing circular holes at different diameter and number. It was observed from this figure that the effectiveness increased with the increase of *NTU*. The effectiveness values of heat exchanger, which used of swirl generators containing holes for the passage of fluid into the tube, varied between 53% with 82% in counter flow mode, 51% with 80% in parallel flow mode. The highest effectiveness was obtained in a counter-flow mode by a swirl generator having 20 circular holes with 3 mm diameter. The increase in the effectiveness value was obtained up to 50–70% compared to a heat exchanger with the empty

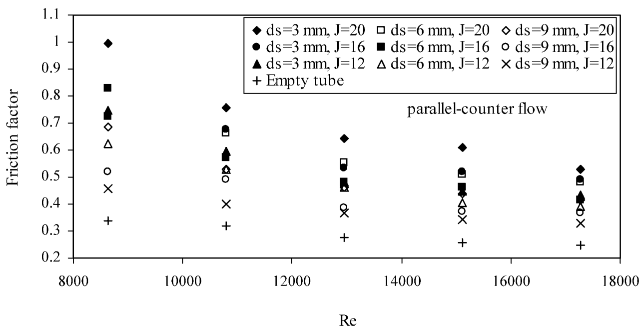

Fig. 5. The variation of friction factor with Reynolds number in the parallel and counter.

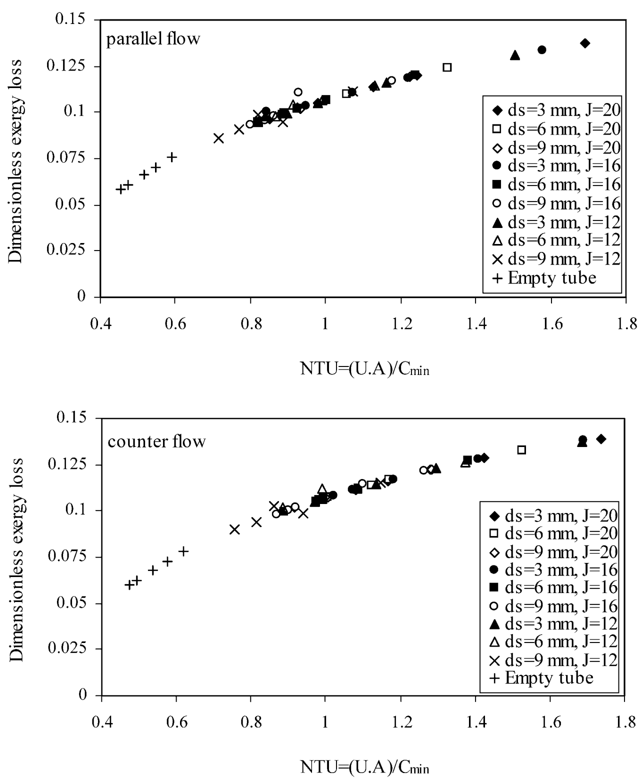

Fig. 6. The variation of dimensionless exergy loss with *NTU* in the parallel and counter.

tube for counter and parallel flow mode. In addition, the effectiveness and *NTU* increased with the increase of holes number and decreased with the increase of the holes diameter.

Pressure drops were found about equal for both flow modes and increased with Reynolds numbers. The friction factors were calculated by using Eq. (25) based on the pressure drops. Friction factors in the inner test pipe are given in Fig. 5 as a function of the Reynolds number, for air side, and various swirl generators containing circular holes at different diameter and number. A great increase in friction factors occurred when swirl flow generator was mounted at inlet of the inner pipe, in comparison with inner pipe entrance without swirl generator. This results mainly from the dissipation of the dynamical pressure of the fluid (i.e., air) due to very

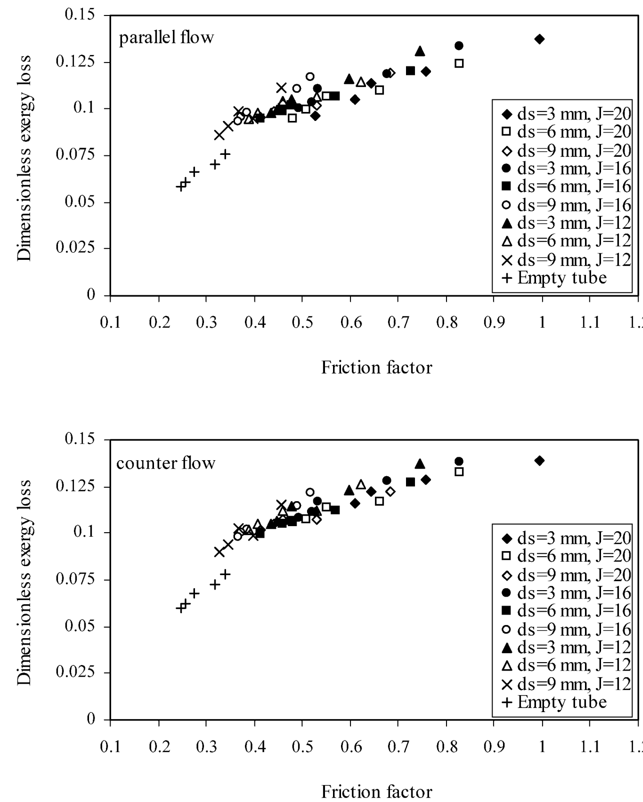

Fig. 7. The variation of dimensionless exergy loss with friction factor in the parallel and counter.

high viscous losses near the pipe wall, and to the extra forces exerted by rotation. Moreover the pressure drop increase is probably due to the secondary flows occurring as a result of the interaction of pressure forces with inertial forces in the boundary layer. It was seen from Fig. 5 that the frictions factors in the inner pipe decreased with the increase of the Reynolds numbers and decreased with the increase of the holes diameter and increased with the increase of holes number. There was increase of up 2.9 times in the friction factor for swirl generator having 20 holes with 3 mm diameter, when it was compared to a heat exchanger with the empty tube.

Fig. 6 shows the changes of the dimensionless exergy loss with *NTU* for various swirl generators containing circular holes at different diameter and number. The exergy loss increased with the increase of *NTU*. In addition, the exegy loss and *NTU* increased with the increase of holes number and decreased with the increase of the holes diameter. The increase was about 1.25 times that of the empty tube at the highest Reynolds number for swirl element having 20 holes with 3 mm diameter.

Variation of the dimensionless exergy loss with frictional factor for various swirl generators is shown in Fig. 7. It can be seen that the dimensionless exergy loss increased with the increase of friction factor. As is know, the irreversibility of any heat exchanger is due to losses of the heat transfer and the frictional pressure drop. Heat transfer losses can be reduced by increasing the heat transfer area, but in this case pressure drops in the pipe increase [26,27].

Linear and non-linear regression models are important tools to find the relationship between different variables, especially, for which no established empirical relation exists. In this study, the empirical relations were derived for the variation of the Nusselt number with the Reynolds number, the variation of effectiveness with *NTU*, the variation of friction factor with the Reynolds number and the variation of the dimensionless exergy loss with *NTU*. Based on the multiple regression analysis, the accepted relations and correlation coefficients, *RMSE* and χ^2 values are given in the following. It was shown that the accepted empirical relations describing values of the heat transfer, the effectiveness, the friction factor and the dimensionless exergy loss of concentric heat exchanger with swirl generator gave very high R-value and low *RMSE* and χ^2 values.

For heat exchanger equipped with swirl generators,

$$Nu = 0.372\, Re^{0.664} Pr^{5.633} \left(\frac{d_\mathrm{i}}{d_\mathrm{s}}\right)^{0.036} j^{0.202}. \tag{28}$$

In parallel flow

$$R = 0.958, \qquad RMSE = 2.754, \qquad \chi^2 = 8.53$$

$$Nu = 0.331\, Re^{0.668} Pr^{4.630} \left(\frac{d_\mathrm{i}}{d_\mathrm{s}}\right)^{0.029} j^{0.144} \tag{29}$$

In counter flow

$$R = 0.948, \qquad RMSE = 3.303, \qquad \chi^2 = 12.28$$

$$\varepsilon = 0.521\, NTU^{0.551} \left(\frac{d_\mathrm{i}}{d_\mathrm{s}}\right)^{-0.033} j^{0.086} \tag{30}$$

In parallel flow

$$R = 0.984, \qquad RMSE = 0.0126, \qquad \chi^2 = 1.75 \times 10^{-4}$$

$$\varepsilon = 0.705\, NTU^{0.520} \left(\frac{d_\mathrm{i}}{d_\mathrm{s}}\right)^{0.024} j^{-0.059} \tag{31}$$

In counter flow

$$R = 0.990, \qquad RMSE = 0.0094, \qquad \chi^2 = 9.78.10^{-5}$$

$$f = 396.867\, Re^{-0.783} \left(\frac{d_\mathrm{i}}{d_\mathrm{s}}\right)^{0.169} j^{0.159} \tag{32}$$

In parallel and counter flow

$$R = 0.819, \qquad RMSE = 0.0826, \qquad \chi^2 = 7.49.10^{-3}$$

$$e = 0.086\, NTU^{0.502} \left(\frac{d_\mathrm{i}}{d_\mathrm{s}}\right)^{0.028} j^{0.057} \tag{33}$$

In parallel flow

$$R = 0.959, \qquad RMSE = 0.0032, \qquad \chi^2 = 1.15 \times 10^{-5}$$

$$e = 0.105\, NTU^{0.504} \left(\frac{d_\mathrm{i}}{d_\mathrm{s}}\right)^{0.0017} j^{0.0047} \tag{34}$$

In counter flow

$$R = 0.990, \qquad RMSE = 0.0016, \qquad \chi^2 = 2.89 \times 10^{-6}$$

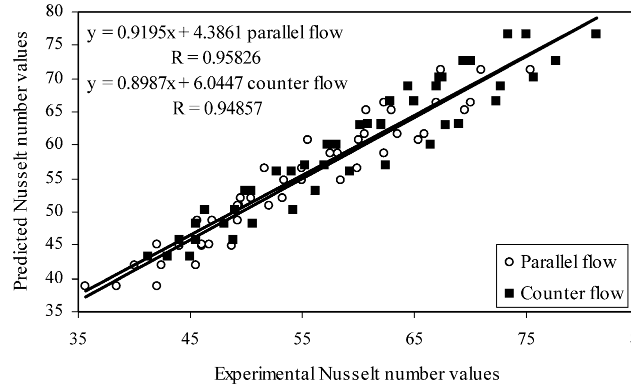

Fig. 8. Comparison of experimental and predicted Nusselt number values by Eqs. (28) and (29).

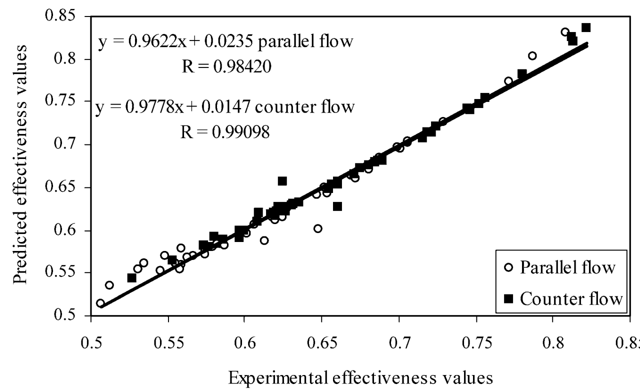

Fig. 9. Comparison of experimental and predicted effectiveness values by Eqs. (30) and (31).

Here, $(d_\mathrm{i}/d_\mathrm{s})$ was selected for obtained a dimensionless value. d_i and d_s are diameter of inner pipe, diameter of holes on the swirl elements, respectively.

The accuracy of the established empirical relations was evaluated by comparing the computed data in any particular experimental conditions with the observed data. The performance of the empirical relationships of the Nusselt number (Eqs. (28), (29)), the effectiveness (Eqs. (30), (31)), the friction factor (Eq. (32)) and the dimensionless exergy loss (Eqs. (33), (34)) at all experimental conditions have been illustrated in Figs. 8–11 for both flow modes. The predicted data generally banded around the straight line which showed the suitability of the empirical relations in describing the Nusselt number, the effectiveness, the friction factor and the dimensionless exergy loss value in any particular experimental conditions. In addition, as seen from Figs. 8–11, measurement results are reasonably close to the empirical results. The causes of the errors between the empirical and the experimental values can be considered because of setting and measurements of temperature, volume flow rate, and the pressure of air in the system under laboratory conditions. If the uncertainties occurred during the measurements of the parameters are decreased; heat transfer losses, pressure drop and irreversibility can be decreased.

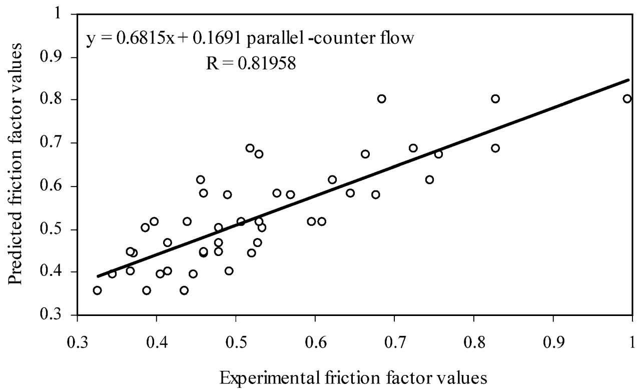

Fig. 10. Comparison of experimental and predicted friction factor values by Eq. (32).

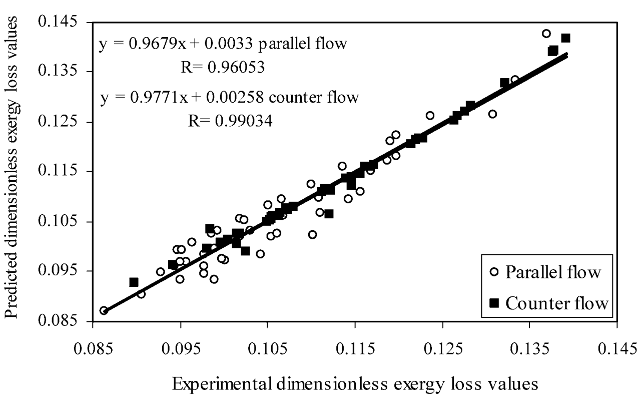

Fig. 11. Comparison of experimental and predicted dimensionless exergy loss values by Eqs. (33) and (34).

7. Conclusions

The present study explored the effect of different swirl generators on the heat transfer, friction factor and dimensionless exergy loss. Key findings from the study may be summarized as follows:

(1) Heat transfer rates increased with decreasing diameter and with increasing number of holes on the swirl generators used in the experiments. The highest enhancement was seen to occur in countercurrent flow mode of the exchanger with swirl generators having 3 mm hole diameter and 20 holes. The heat transfer rates in this heat exchanger increased up to 130% by giving rotation to the air with the help of the swirl elements.

(2) The effectiveness values of heat exchanger which used swirl generators containing holes for the passage of fluid into the tube was obtained up to 70–80% compared to a heat exchanger with the empty tube for counter and parallel flow mode.

(3) Swirl generators caused a considerable increase in pressure drop and friction factor. In the case of both counter and parallel flow mode, the average increase friction factors at the highest Reynolds number for swirl element having 20 holes with 3 mm diameter was about 2.9 times in comparison with that for the inner pipe without swirl generators.

(4) The dimensionless exergy loss and *NTU* increased with the increase of holes number and decreased with the increase of the holes diameter. The increase was about 1.25 times that of the empty tube at the highest Reynolds number for swirl element having 20 holes with 3 mm diameter. When the increase at dimensionless exergy loss is compared with the increase at heat transfer, a counter flow heat exchanger with swirl generator was determined to be more advantageous.

(5) The dimensionless exergy loss increased with the increase of friction factor.

References

[1] A.E. Bergles, Heat transfer enhancement-the encouragement and accommodation of high heat fluxes, J. Heat Transfer (Trans. ASME) 119 (1997) 8–19.
[2] M. Yilmaz, O. Comakli, S. Yapici, O.N. Sara, Heat transfer and friction characteristics in decaying swirl flow generated by different radial guide vane swirl generators, Energy Convers. Management 44 (2003) 283–300.
[3] A. Durmus, Heat exchanger and exergy loss in a concentric heat exchanger with snail entrance, Internat. Commun. Heat Mass Transfer 29 (3) (2002) 303–312.
[4] A. Durmus, Heat transfer and exergy loss in cut out conical turbulators, Energy Convers. Management 45 (5) (2004) 785–796.
[5] I. Dincer, Thermodynamic, exergy and environmental impact, Energy Sources 22 (8) (2000) 723–732.
[6] I. Dincer, A.Z. Sahin, A new model for thermodynamic analysis of a drying process, Internat. J. Heat Mass Transfer 47 (4) (2004) 645–652.
[7] S. Ito, K. Ogawa, C. Kuroda, Static-pressure distribution for swirling flow in a cylindrical pipe, Internat. Chem. Engrg. 22 (1982) 295–300.
[8] E.M. Sparrow, A. Chaboki, Swirl affected turbulent fluid flow and heat in a circular tube, ASME Heat Transfer 106 (1984) 766–773.
[9] A.H. Algifri, R.K. Bhardwaj, Prediction of heat transfer in decaying turbulent swirl flow in a tube, Internat. J. Heat Mass Transfer 28 (1985) 1637–1643.
[10] A.H. Algifri, R.K. Bhardwaj, Y.V.N. Rao, Heat transfer in turbulent decaying swirl flow in a circular pipe, Internat. J. Heat Mass Transfer 31 (1988) 1563–1568.
[11] M. Yilmaz, O. Comakli, S. Yapici, Enhancement of heat transfer by turbulent decaying swirl flow, Energy Convers. Management 40 (1999) 1365–1376.
[12] A. Durmus, A. Durmus, M. Esen, Investigation of heat transfer and pressure drop in a concentric heat exchanger with snail entrance, Appl. Therm. Engrg. 22 (2002) 321–332.
[13] E.K. Akpinar, Y. Bicer, C. Yildiz, D. Pehlivan, Heat transfer enhancements in a concentric double pipe exchanger equipped with swirl elements, Internat. Commun. Heat Mass Transfer 31 (6) (2004) 857–868.
[14] S. Martemianov, V.L. Okulov, On heat transfer enhancement in swirl pipe flows, Internat. J. Heat Mass Transfer 47 (2004) 2379–2393.
[15] M.A. Rosen, I. Dincer, Effect of varying dead-state properties on energy and exergy analyses of thermal systems, Internat. J. Thermal Sci. 43 (2) (2004) 121–133.
[16] M. Kanoglu, M.Ö. Carpinlioglu, M. Yildirim, Energy and exergy analyses of an experimental open-cycle desiccant cooling system, Appl. Therm. Engrg. 24 (2004) 919–932.
[17] M. Bayrak, A. Midilli, K. Nurveren, Energy and exergy analyses of sugar production stages, Internat. J. Energy Res. 27 (2003) 989–1001.

[18] A. Midilli, H. Kucuk, Energy and exergy analyses of solar drying process of pistachio, Energy 28 (2003) 539–556.

[19] S. Syahrul, F. Hamdullahpur, I. Dincer, Exergy analysis of fluidized bed drying of moist particles, Exergy Internat. J. 2 (2002) 87–98.

[20] E. Paykoc, H. Yüncü, Irreversibility in double pipe exchangers, TIBTD (Turkish J.) 9 (3) (1986) 35–41.

[21] E. Akpinar, A. Midilli, Y. Bicer, Single layer drying behavior of potato slices in a convective cyclone dryer and mathematical modeling, Energy Convers. Management 44 (2003) 1689–1705.

[22] J.P. Holman, Experimental Methods for Engineers, McGraw–Hill, Singapore, 1994.

[23] C. Yildiz, Y. Bicer, D. Pehlivan, Effect of twisted strips on heat transfer and pressure drop in heat exchangers, Energy Convers. Management 39 (3/4) (1998) 331–336.

[24] C. Yildiz, Y. Bicer, D. Pehlivan, Heat transfer and pressure drop in a heat exchanger with a helical pipe containing inside springs, Energy Convers. Management 38 (6) (1997) 619–624.

[25] I. Dincer, The role of exergy in energy policy making, Energy Policy 30 (2002) 137–149.

[26] R.T. Ogulata, F. Doba, T. Yilmaz, Second-law and experimental analysis of a cross-flow heat exchanger, Heat Transfer Engrg. 20 (2) (1999) 20–27.

[27] R.T. Ogulata, F. Doba, Experiments and entropy generation minimization analysis of a cross-flow heat exchanger, Internat. J. Heat Mass Transfer 41 (2) (1998) 373–381.

[28] A. Bejan, Advanced Engineering Thermodynamics, Wiley, New York, 1988.

[29] Y.A. Cengel, Heat Transfer: A Practical Approach, second ed., McGraw–Hill, New York, 1998.